


RESEARCH ARTICLE

Sex-Specific Effects of Cholesteryl Ester Transfer Protein (CETP) on the Perivascular Adipose Tissue

C.M. Lazaro ¹, I.N. Freitas¹, V.S. Nunes², D.M. Guizoni³, J.A. Victorio⁴,
H.C.F. Oliveira^{1,3,*}, A.P. Davel^{1,3,*}

¹Departamento de Biologia Estrutural e Funcional, Instituto de Biologia, Universidade Estadual de Campinas (UNICAMP), CEP 13083-862, Campinas, SP, Brazil, ²Laboratório de Lípidos (LIM10), Hospital das Clínicas (HCFMUSP) da Faculdade de Medicina da Universidade de São Paulo, CEP 01246-903, São Paulo, SP, Brazil, ³Obesity and Comorbidities Research Center, Universidade Estadual de Campinas (UNICAMP), CEP 13083-864, Campinas, SP, Brazil and ⁴Laboratory of Female Vascular Biology, Departamento de Ciências Fisiológicas, Centro de Ciências Biológicas, Universidade Federal de Santa Catarina (UFSC), CEP 88037-000, Santa Catarina, SC, Brazil

*Address correspondence to H.C.F.O. (e-mail: ho98@unicamp.br) and A.P.D. (e-mail: anadavel@unicamp.br).

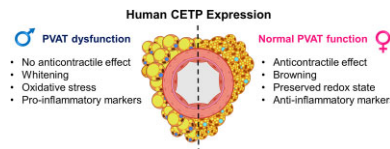
Article type: Research Article

Abstract

Cholesteryl ester transfer protein (CETP) increases the atherosclerosis risk by lowering HDL-cholesterol levels. It also exhibits tissue-specific effects independent of HDL. However, sexual dimorphism of CETP effects remains largely unexplored. Here, we hypothesized that CETP impacts the perivascular adipose tissue (PVAT) phenotype and function in a sex-specific manner. PVAT function, gene and protein expression, and morphology were examined in male and female transgenic mice expressing human or simian CETP and their non-transgenic counterparts (NTg). PVAT exerted its anticontractile effect in aortas from NTg males, NTg females, and CETP females, but not in CETP males. CETP male PVAT had reduced NO levels, decreased eNOS and phospho-eNOS levels, oxidative stress, increased NOX1 and 2, and decreased SOD2 and 3 expressions. In contrast, CETP-expressing female PVAT displayed increased NO and phospho-eNOS levels with unchanged NOX expression. NOX inhibition and the antioxidant tempol restored PVAT anticontractile function in CETP males. *Ex vivo* estrogen treatment also restored PVAT function in CETP males. Moreover, CETP males, but not female PVAT, show increased inflammatory markers. PVAT lipid content increased in CETP males but decreased in CETP females, while PVAT cholesterol content increased in CETP females. CETP male PVAT exhibited elevated leptin and reduced Prdm16 (brown adipocyte marker) expression. These findings highlight CETP sex-specific impact on PVAT. In males, CETP impaired PVAT anticontractile function, accompanied by oxidative stress, inflammation, and whitening. Conversely, in females, CETP expression increased NO levels, induced an anti-inflammatory phenotype, and preserved the anticontractile function. This study reveals sex-specific vascular dysfunction mediated by CETP.

Submitted: 16 January 2024; Revised: 8 May 2024; Accepted: 13 May 2024

© The Author(s) 2024. Published by Oxford University Press on behalf of American Physiological Society. This is an Open Access article distributed under the terms of the Creative Commons Attribution-NonCommercial License (<https://creativecommons.org/licenses/by-nc/4.0/>), which permits non-commercial re-use, distribution, and reproduction in any medium, provided the original work is properly cited. For commercial re-use, please contact journals.permissions@oup.com



Key words: CETP; perivascular adipose tissue; oxidative stress

Introduction

Perivascular adipose tissue (PVAT) surrounds most blood vessels and is considered a fourth layer of the arterial wall.¹ PVAT can synthesize and release various autocrine and paracrine factors, such as adipokines, many of which possess vasoactive properties. In a healthy state, thoracic aortic PVAT secretes anti-inflammatory adipokines and nitric oxide (NO), promoting vasodilation and maintaining vascular homeostasis, thus assisting the prevention of cardiovascular diseases (CVD).^{2,3} The anti-contraction function from PVAT was first demonstrated in rat thoracic aorta,⁴ and then confirmed in mouse⁵ and human vessels.⁶ PVAT from large arteries, such as the thoracic aorta, is characterized by a predominance of brown adipocytes, typically expressing thermogenic genes, including *Ucp-1*, *Prdm16*, and *Cidea*, while less white adipocytes are found in comparison to abdominal PVAT.^{7,8}

Cholesteryl ester transfer protein (CETP) is a hydrophobic glycoprotein secreted by many tissues, mainly liver and adipose tissue.^{9,10} Plasma CETP facilitates the transfer of esterified cholesterol from HDL to VLDL and LDL in exchange for triglycerides, ultimately reducing the plasma levels of HDL-cholesterol.¹¹ HDL particles have well-characterized antiatherogenic effects, including driving cholesterol to hepatic excretion, stimulating endothelial NO release, anti-inflammatory, antioxidant, and anti-thrombotic effects.¹² Because CETP reduces HDL cholesterol, it is considered a pro-atherogenic protein. CETP transgenic mouse models have been useful to study atherosclerosis susceptibility. Experimental evidence from these genetically modified mice supports the concept that CETP is indeed pro-atherogenic when expressed in a hyperlipidemic atherosclerosis-prone background, such as the *Ldl* receptor or *Apoe* knockout mice. On the other hand, CETP may have a protective role against atherosclerosis in conditions where LDL receptor function is preserved, even in the presence of other risk factors.¹³ In addition, CETP may have tissue-specific HDL-independent local effects such as anti-adipogenic,^{14,15} anti-inflammatory,^{16–18} and antioxidant.¹⁹

Studies focusing on CETP have rarely compared both sexes. In adult (premenopausal) women, plasma CETP activity has been reported to be higher than in men.^{20,21} Interestingly, CETP expression protects female but not male mice from high-fat diet-induced insulin resistance by increasing muscle glycolysis²² and reducing hepatic glucose production.²³ Therefore, CETP seems to have beneficial metabolic effects on females. We previously reported contrasting sex effects of CETP on the aorta vascular reactivity in transgenic mice. Male CETP mice showed impaired endothelium-mediated vascular relaxation, which was associated with vascular oxidative stress.²⁴ Conversely, female CETP mice displayed preserved endothelium-dependent relaxation, reduced vasocontractile response, and improved relaxation response to 17β -estradiol (E₂).²⁵ However, these previous studies were conducted in aorta without PVAT.

PVAT dysfunction is characterized by an adipokine profile shift towards a pro-inflammatory and vasoconstrictive type, often present in pathological conditions such as obesity, insulin resistance, hypertension, and atherosclerosis.^{1,26} The altered adipokine profile impairs PVAT anticontractile properties through macrophage activation, inflammatory cytokine release, and ROS production.^{26,27} Although CETP activity modulates plasma lipid metabolism and cardiovascular risk, it remains unclear whether CETP expression could modify PVAT phenotype and function in a sex-specific manner. Hence, the present study aims to investigate CETP effects on the PVAT function of male and female transgenic mice and explore underlying mechanisms.

Materials and Methods

Animals

All experimental procedures were approved by the Committee for Ethics in Animal Experimentation of the State University of Campinas (CEUA/UNICAMP; protocols #5105-1/2019 and #6010-1/2022). These experiments follow the ethical principles of the National Council for the Control of Animal Experimentation (CONCEA, Brazil) and conform to the ARRIVE (Animal Research: Reporting of *In Vivo* Experiments) guidelines. Male and female mice, aged 4–6 months, were housed in a temperature-controlled conventional room, maintained at $22 \pm 2^\circ\text{C}$, with a 12-h light/dark cycle, and 15 air changes per hour. The mice had free access to filtered water and were fed a standard laboratory rodent chow diet (Nuvital CR1, Colombo, Brazil). We utilized hemizygous CETP transgenic (Tg) mice, which expressed a human CETP transgene driven by its natural promoter (line 5203, The Jackson Laboratory, Bar Harbor, ME, USA, RRID: 4 IMSR.JAX:003 904), as well as mice expressing a simian CETP transgene controlled by the mouse metallothionein (MT1) promoter (The Jackson Laboratory, Bar Harbor, ME, USA, RRID: IMSR.JAX:001 929). These mice were maintained at UNICAMP through crossbreeding with C57BL6/JUnib mice (RRID: MGI:7 264 953, Multidisciplinary Center for Biological Investigation on Laboratory Animal Science, CEMIB/UNICAMP, Campinas, Brazil) to generate human CETP-Tg (hCETP) (>20 generations), simian CETP-Tg (sCETP) (>8 generations), and non-transgenic (NTg) littermate controls. CETP genotyping was performed using polymerase chain reaction (PCR) with tail tip DNA following the Jackson Laboratory protocols. Mice were anesthetized with isoflurane (Cristália, Águas de Lindóia, Brazil) and decapitated. Body weights of mice in the present study were not affected by the CETP expression regardless of sex (males: NTg = 29 ± 1 vs. hCETP = 28 ± 1 g, $P = .408$; females: NTg = 25 ± 1 vs. hCETP = 25 ± 1 g, $P = .999$).

The influence of estrous cycle phase on the PVAT anticontractile function was determined in a separated cohort. The estrous cycle was monitored daily through vaginal smears collected between 8:00 and 9:00 AM and observed under light microscopy.

Anticontractile Effect of Aortic PVAT

The thoracic aorta was immersed in ice-cold Krebs–Henseleit solution (KHS) containing the following concentrations (in mM): 118 NaCl, 4.7 KCl, 2.5 CaCl₂·2H₂O, 1.2 KH₂PO₄, 1.2 MgSO₄·7H₂O, 25 NaHCO₃, 11 glucose, and 0.01 EDTA, adjusted to a pH of 7.4. Aortic rings, measuring 3 mm in length, were prepared with intact perivascular adipose tissue (PVAT+) or with PVAT carefully removed using ophthalmic scissors on a microscope (PVAT–).²⁸ Isometric tension was measured using a force transducer (MLT0420, AD Instruments, Sydney, Australia) connected to a PowerLab 8/30 data acquisition system (LabChart 7, AD Instruments, Sydney, Australia). Aortas were exposed to potassium chloride (100 mM KCl) to confirm the integrity of smooth muscle and establish maximum contraction responses. Subsequently, the aortic rings were rinsed with KHS, and relaxation responses to acetylcholine (ACh, 0.1 nM to 30 μM) or sodium nitroprusside (SNP, 0.01 nM to 10 μM) were assessed in PVAT– and PVAT+ aortic rings pre-contracted with the thromboxane A₂ analogue U-46619 (to reach a contraction level of 50–70% of the maximum induced by 100 mM KCl). Contraction response to phenylephrine (PE, 0.1 nM to 10 μM) was investigated in both PVAT+ and PVAT– rings. Additional experiments were performed using the NOX inhibitor diphenyleiodonium (DPI, 10 μM) for 30 min, NOX-2-specific inhibitor GSK2795039 (GSK, 25 μM) for 30 min, the antioxidant Tempol (100 μM) for 30 min, and E2 (10 μM) for 1 h. Vehicles of DPI, GSK, and E2 (DMSO) had no effect on contraction in both groups (data not shown) and Tempol where diluted in distilled water. All drugs were obtained from Sigma-Aldrich, Saint Louis, MO, USA. Potency (LogEC₅₀) and maximum response (Emax) to the agonists at each concentration-response curve were calculated using GraphPad Prism® 7.

Plasma Lipoprotein Profile and CETP Activity

Plasma lipoproteins were isolated by fast protein liquid chromatography (FPLC) using an AKTA Purifier Liquid Chromatography System (Cytiva, Marlborough, MA, USA). A total of 100 μL of plasma was injected onto an HR10/30 Superose 6 column and elution was performed at a constant flow rate of 0.5 mL/min using tris buffer (10 mM Tris, 150 mM NaCl, 1 mM EDTA, and 0.03% NaN₃, pH 7.0). Fractions of 0.2 mL were collected in 96-well plates. Cholesterol levels from 60 fractions were determined using an enzymatic-colorimetric method (Labtest Diagnostica, Lagoa Santa, Minas Gerais, Brazil), following the manufacturer's instructions. This process allowed for the identification of the peaks corresponding to VLDL (fractions 10–25), LDL + IDL (fractions 26–40), and HDL (fractions 41–60). CETP activity in plasma samples was measured using a commercial fluorometric assay following the manufacturer's instructions (CETP Activity Assay Kit, MAK106, Sigma-Aldrich, Saint Louis, MO, USA).

PVAT Nitric Oxide (NO) and Reactive Oxygen Species (ROS) Levels

Transverse PVAT slices measuring 15 μm in thickness were obtained from OCT frozen tissue (Optimal Cutting Temperature Compound, Tissue-Tek, Sakura Finetek, Torrance, CA, USA) using a cryostat (Leica CM1860, Leica Biosystems, Nußloch, Heidelberg, Germany) set at –20°C. For NO content analysis, PVAT slices were incubated in phosphate-buffered saline (PBS) supplemented with CaCl₂ (0.45 mM), pH = 7.5, 37°C, for 10

min. Subsequently, the tissues were treated with the probe 4,5-diaminofluorescein diacetate (DAF-2DA, 8 μM, Sigma-Aldrich, Saint Louis, MO, USA) for 30 min. Tissues were further incubated with DAPI (5 min, 1:5000, Sigma-Aldrich, Saint Louis, MO, USA) to stain the cell nuclei. For ROS analysis, PVAT slices were first incubated in PBS, pH = 7.5, 37°C, for 10 min and then exposed to dihydroethidium (DHE, 2 μM, Sigma-Aldrich, Saint Louis, MO, USA) for 30 min, which becomes fluorescent when oxidized. Some PVAT slices were incubated with N(G)-Nitro-L-arginine methyl ester (L-NAME, 1 mM, Sigma-Aldrich, Saint Louis, MO, USA) to assess the involvement of nitric oxide synthase (NOS). Images were captured in a microscope (Nikon Eclipse, Shinagawa, Tokyo, Japan) equipped with a fluorescence reader using a 20× objective. Subsequently, these images were analyzed using the ImageJ software, version 1.53k (US National Institutes of Health, Bethesda, MD, USA, <http://imagej.nih.gov/ij>).

PVAT Gene Expression

Thoracic aorta and adjacent PVAT (10 mg) were used separately to extract total RNA. Tissues were disrupted using stainless steel beads of 5 mm diameter in a TissueLyser LT (Qiagen 85 600, Venlo, The Netherlands). The resulting tissue homogenates were purified using the RNeasy Plus Mini Kit (Qiagen 74 134, Venlo, The Netherlands). The total RNA was quantified using a NanoDrop™ 2000/2000c spectrophotometer (ThermoFisher Scientific, Waltham, MA, USA) and 1 μg was reverse transcribed using the High-Capacity cDNA Reverse Transcription Kit (ThermoFisher Scientific 4 368 814, Waltham, MA, USA) and a GeneAmp PCR System 9700 device (Applied Biosystems, Foster City, CA, USA). Reverse transcription was performed in four steps: 25°C for 10 min, 37°C for 120 min, 85°C for 5 min, and then maintenance at 4°C. Target gene amplification was carried out using Fast SYBR Green Master Mix (ThermoFisher Scientific 4 385 612, Waltham, MA, USA) or QuantiNova SYBR Green PCR kit (Qiagen 208 054, Venlo, The Netherlands). cDNA (200 ng) and forward and reverse oligonucleotide primers (300 nM) (Supplementary Table S1) were used for the reaction carried out in the 7500 Fast Real-Time PCR System (Applied Biosystems, Foster City, CA, USA), following the steps: 95°C for 20 s, and 40 cycles of denaturation at 95°C for 3 s and annealing/extension at 60°C for 30 s. Gene expression was normalized using the internal control Rplp0 (ribosomal protein lateral stalk subunit P0), and the relative abundance of mRNA was quantified using the threshold cycle method (ΔΔCT).

PVAT Western Blot

Frozen thoracic aorta PVAT samples were pulverized and homogenized in cold RIPA lysis buffer containing phenylmethylsulfonyl fluoride (1 mM PMSF), Na₃VO₄ (10 mM), and a protease inhibitor cocktail. The protein extracts (30 μg) were then separated by SDS-PAGE (7.5%) and transferred to PVDF membranes (GE HealthCare, Chicago, IL, USA), with a Mini Trans-Blot Cell System (Bio-Rad, Hercules, CA, USA) containing 25 mM Tris, 190 mM glycine, 20% methanol, and 0.05% SDS. The membranes were blocked (90 min) with 5% albumin in Tris buffer (10 mM Tris, 100 mM NaCl, and 0.1% Tween 20) and incubated overnight at 4°C with primary antibodies: anti-eNOS (1:500, 610297, BD, Franklin Lakes, NJ, USA), anti-phospho-eNOS at Serine1177 (1:500, AB75639, Abcam, Cambridge, UK), and β-actin as internal control (1:1000, 8H10D10, Cell Signaling, Danvers, MA, USA). After washing, membranes were incubated (90 min)

with secondary antibodies conjugated with horseradish peroxidase. Immunocomplexes were detected using an enhanced horseradish peroxidase-luminol detection system (Pierce ECL Western 32 106, ThermoFisher Scientific, Waltham, MA, USA), and band intensities were quantified using the ImageJ software, version 1.53k (US National Institutes of Health, Bethesda, MD, USA, <http://imagej.nih.gov/ij>).

Histological Analysis

Segments of thoracic aorta PVAT were fixed in 10% buffered formalin for 24 h. Subsequently, the tissues were washed and kept in 70% alcohol, and later embedded in paraffin (Sigma-Aldrich, Saint Louis, MO, USA). Tissues were sliced (5 μ m sections) using an automatic microtome (LEICA RM 2155, Leica Biosystems, Nußloch, Heidelberg, Germany) and stained with hematoxylin and eosin (Sigma-Aldrich, Saint Louis, MO, USA). Sections were then dehydrated and mounted on glass slides with entellan (Merck, Saint Louis, MO, USA) for image capturing with an optical microscope (Nikon Eclipse, Shinagawa, Tokyo, Japan) at 20 \times magnification. The images were quantified using the ImageJ software, version 1.53k (US National Institutes of Health, Bethesda, MD, USA, <http://imagej.nih.gov/ij>). The percentage of fat present in the section area was quantified using the method of Parlee and colleagues.²⁹

PVAT Cholesterol Content

PVAT cholesterol content was assessed using gas chromatography coupled with mass spectrometry (GCMS) (Shimadzu GCMS-QP2010 Plus, Kyoto, Japan) and GCMS solution software, version 2.5, as previously described.³⁰ Lipids were extracted using chloroform:methanol (2:1), and an internal standard (5- α -cholestane) was added to the lipid extracts. Saponification was carried out with 1 mL of 1 M KOH dissolved in ethanol at 60°C for 1 h. Afterward, 1 mL of water was added, and the mixture was extracted twice with hexane. The hexane phase was dried under nitrogen and derivatized using a solution consisting of pyridine (100 μ L) and BSTFA with 1% TMCS (1:1, v/v), followed by incubation for 1 h at 60°C. A one-microliter sample was then injected into the GCMS equipment with a split ratio of 1:3. Sterol separation occurred within a Restek capillary column (100% dimethyl polysiloxane-Rxi13323) measuring 30 m in length and 0.25 mm in internal diameter. Helium served as the mobile phase, maintaining a constant linear velocity of 45.8 cm/s, with an oven temperature held at 280°C. The mass spectrometer operated in the electron impact mode at an ionization voltage of 70 eV, with a source temperature of 300°C for the ions and the interface. Ion monitoring was conducted in SIM mode (single ion monitoring), with selected ions at $m/z = 217, 149, \text{ and } 109$ for 5- α -cholestane and $m/z = 121, 129, \text{ and } 329$ for cholesterol. Quantitation relied on the total ion chromatogram (TIC) and identification was based on the comparison with retention times and mass spectra of standards, adjusted for the internal standard, and tissue mass.

Statistical Analysis

The data are expressed as mean \pm standard error (SE) and were analyzed using GraphPad Prism[®]7 software. Outliers were identified and removed using the Grubb's test ($\alpha = 0.05$). The normal distribution of the data was tested with Shapiro-Wilk test, and parametric or non-parametric statistical tests were chosen

depending on the data distribution. Student's t-test or Mann-Whitney was employed to compare two experimental groups, and two-way ANOVA with Sidak's post-test was used for multiple comparisons in concentration-response curves. $P \leq .05$ was considered statistically significant.

Results

CETP Expression Impairs PVAT Function in Male But Not in Female Mice

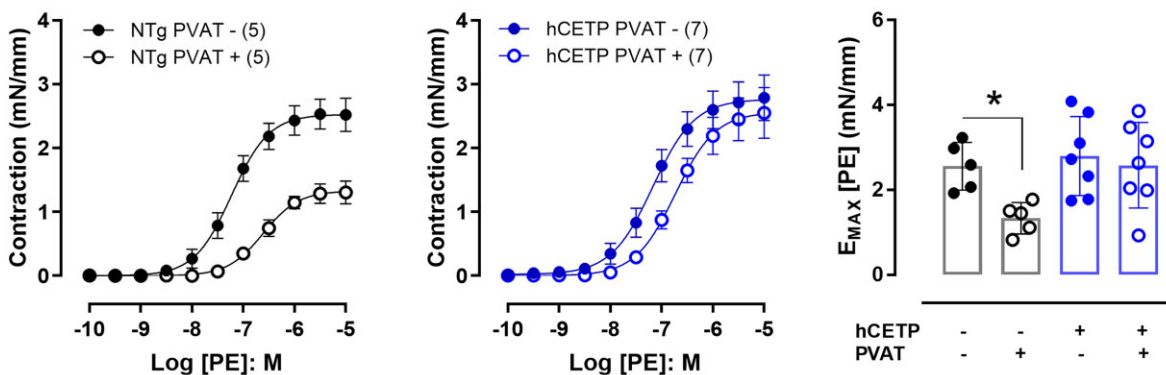
The anticontractile effect of PVAT from thoracic aorta was evaluated by the reduction in the maximal contraction (E_{max}) to phenylephrine (PE) in NTg male and NTg female mice (Figure 1A and B). In male mice expressing human CETP (hCETP), this anticontractile effect of PVAT was impaired (Figure 1A), while it was preserved in the aorta from hCETP females (Figure 1B). This indicates that the expression of hCETP affects PVAT function in a sex-specific manner. To confirm these results, we evaluated aorta contraction to PE in an independent line of transgenic mice expressing simian CETP (sCETP). Similar to the hCETP, sCETP male mice showed impaired anticontractile function of PVAT compared to NTg (Supplementary Figure S1A), whereas aorta with PVAT from sCETP female mice exhibited a preserved anticontractile effect (Supplementary Figure S1B). No differences were observed in the PVAT effect on the aorta relaxation response to ACh or SNP in both hCETP and sCETP lines and in both sexes (Supplementary Figure S2). The anticontractile function of PVAT was similar in estrus and diestrus phases in both NTg control and CETP female mice (Supplementary Figure S3).

Next, we evaluate the plasma phenotype of CETP-transgenic mice of both sexes. As expected, plasma CETP activity and aortic and PVAT CETP mRNA were detected only in male and female hCETP transgenic mice (Figure 2A). Lipoprotein profile showed reduced HDL-cholesterol and no changes in VLDL and LDL in both sexes of hCETP mice (Figure 2B). Since sCETP transgenic mice carry a high transgene copy number,³¹ they show a stronger phenotype, that is, high CETP activity (~ 300 pmoles) (Supplementary Figure S4A and C) and marked reductions in HDL-cholesterol and enhanced LDL-cholesterol levels in both male and female sCETP mice (Supplementary Figure S4B and D). These results suggest that the sex differences found in PVAT function in both lines of transgenic mice expressing CETP do not depend on their lipoprotein profiles.

PVAT Dysfunction in Males Expressing CETP is Associated with Reduced NO Production and Oxidative Stress

PVAT-derived NO is important for regulating vascular tone and atheroprotection.^{28,32} Here, we observed a 25% reduction in NO levels (DAF-2DA) in male hCETP PVAT, accompanied by reduced eNOS (Nos3) mRNA (Figure 3A) and total- and phospho-eNOS protein expression (Figure 3B). In contrast, female hCETP PVAT showed a 43% increase in NO levels, without changes in eNOS mRNA expression (Figure 3C) and increased phospho-eNOS levels (Figure 3D). As eNOS uncoupling is a mechanism involved in PVAT dysfunction associated with reduced NO and increased ROS,^{33,34} we investigated the ROS production sensitive to the NOS inhibitor L-NAME. We found an increase in DHE fluorescence, indicative of ROS production, in PVAT from hCETP male mice, that was abolished by the presence of L-NAME (Figure 4A). In contrast, no changes in DHE were found in the PVAT of hCETP female mice (Figure 4C). NADPH oxidases (NOX) are important

A Male



B Female

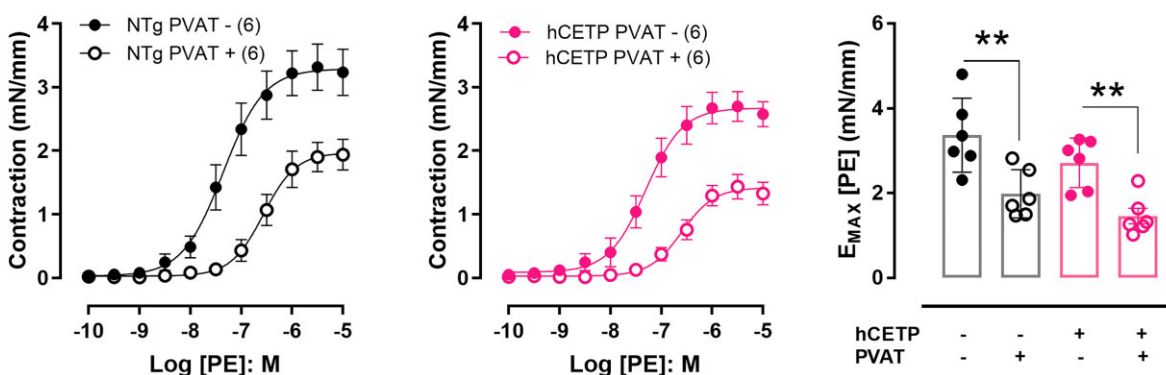


Figure 1. CETP expression impairs the anticontractile effect of PVAT in male but not in female mice. Concentration-response curves to phenylephrine (PE) in aortas with (PVAT+, empty circles) or without PVAT (PVAT-, filled circles) from male NTg to hCETP mice (A) and from female NTg to hCETP mice (B). PE-induced contraction is expressed as millinewton (mN) per aorta length in millimeters (mm). Bar graphs represent maximum responses (E_{max}) to PE in males (A) and females (B). Data are mean \pm SE; the number of animals in each group is in parenthesis. * $P \leq .05$ and ** $P \leq .01$ by ANOVA two-way.

sources of ROS and decrease NO bioavailability. Accordingly, the gene expression of NOX-1 and 2 is enhanced in the PVAT of hCETP male, but not in hCETP female mice (Figure 4B and D). The mRNA levels of superoxide scavenger enzymes superoxide dismutase (SOD) 1 and 2 were reduced in males, while SOD2 expression was higher in hCETP female mice (Figure 4B and D).

To evaluate the contribution of NOXs and overall oxidative stress to the PVAT dysfunction in hCETP males, we used NOX inhibitors, DPI and GSK2795039, and the SOD mimetic Tempol (Figure 4E and F). In NTg males, the incubation of aorta rings with DPI, GSK, and Tempol did not affect the anticontractile effect of PVAT, while DPI, GSK, and Tempol treatments restored the anticontractile function of PVAT in hCETP males (Figure 4E and F). These data indicate that inhibiting ROS-generating enzymes or scavenging ROS with a general antioxidant it is possible to correct PVAT dysfunction in male CETP mice. We also verified that *ex vivo* pretreatment with estradiol restored the anticontractile function of PVAT in hCETP males (Figure 4E and F).

Sex Differences in PVAT Inflammation, Phenotype, and Adipose Markers in Response to CETP Expression

Oxidative stress and inflammation in PVAT are related to vascular dysfunction.³⁵ We thus examined the gene expression of inflammatory markers within the PVAT. In hCETP

males, we observed a reduction in total macrophage Cd68 marker (–17%), reduced anti-inflammatory M2 macrophage marker Cd163 (–16%), increased proinflammatory cytokine TNF α (+93%), and reduced anti-inflammatory IL-10 (–39%) and Arg-1 (–30%) gene expression (Figure 5A). Conversely, hCETP female PVAT showed a reduction in the expression of proinflammatory M1 macrophage markers (–25% in Cd11c/*Itgax* and –29% in Cd80) and increased gene expression of the anti-inflammatory IL-10 (+43%) and Arg-1 (+46%) (Figure 5B).

We also examined adipose histology, lipid and cholesterol content, and gene expression in the aortic PVAT of both sexes. As expected, thoracic-aortic PVAT resembles the phenotype of brown adipocytes.³⁶ However, aortic PVAT of hCETP male mice exhibit larger lipid droplets, whereas hCETP female PVAT showed a reduction in lipid content when compared with their sex-matched NTg PVAT (Figure 6A and B). The cholesterol content in PVAT was higher in hCETP females compared to NTg, while no significant differences in cholesterol content were observed in hCETP males (Figure 6A and B). The reduction in adiposity accompanied by an increase in cholesterol content in the female hCETP PVAT was similar to what was previously observed in the brown adipose tissue of female hCETP mice.¹⁵ Thoracic PVAT total mass was not significantly modified by hCETP expression in both sexes (males: NTg = 26.5 \pm 2.5 vs. hCETP = 31.3 \pm 4.1 mg, $P = 0.336$; females: NTg = 25.6 \pm 3.2 vs. hCETP = 20.2 \pm 1.7 mg, $P = 0.171$).

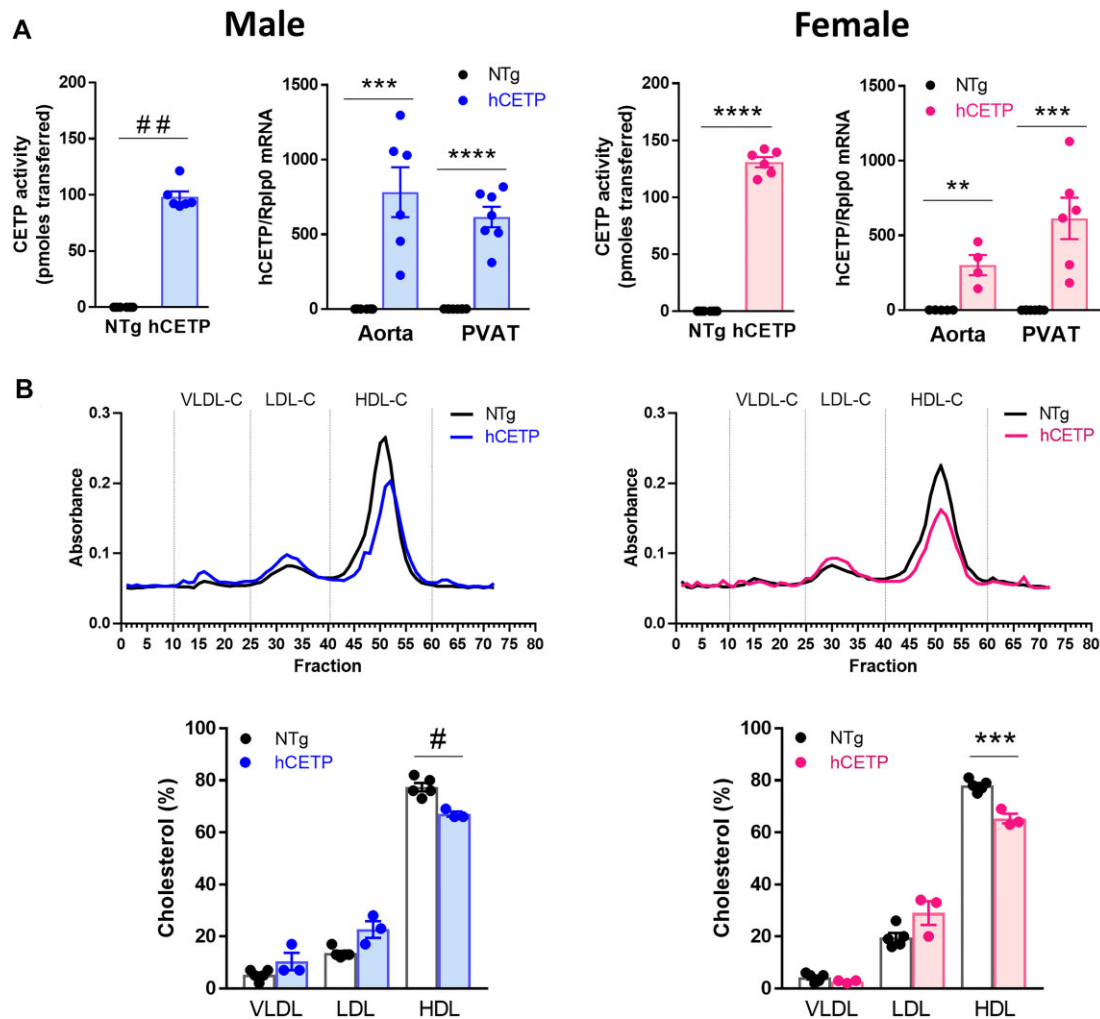


Figure 2. Male and female hCETP-transgenic mice present similar phenotypes. Plasma CETP activity and hCETP mRNA expression in aorta and PVAT from males to females (A). Plasma lipoprotein profile and quantification in male and female NTg, male and female hCETP mice (B). Bars show mean \pm SE of individual values. ** $P \leq .01$, *** $P \leq .001$, and **** $P \leq .0001$ by Student's t-test. # $P \leq .05$ and ## $P \leq .01$ by Mann-Whitney.

The phenotypic change in hCETP male PVAT was accompanied by a marked increase in the expression of the gene encoding *Leptin* (+86%) and a decrease in the brown adipocyte markers *Prdm16* (-33%) and *Cidea* (-39%) (Figure 6C). hCETP female PVAT showed only a reduction in *Cidea* (-32%). Expression of various genes involved in lipid accumulation and depletion did not vary in response to CETP expression regardless the sex (Supplementary Figure S5 A and B). The same is observed for genes encoding sex hormone receptors, as CETP expression did not alter their expression in PVAT of male and female mice (Supplementary Figure S5 A and B).

Discussion

The predominance of males in clinical, epidemiological, experimental, and behavioral studies can introduce biases or ambiguous responses in the investigation targets.³⁷ We previously reported a sexual dimorphism in the endothelial dependent vascular reactivity and vascular redox status in mice expressing CETP.^{24,25} The aorta of male CETP transgenic mice exhibited impaired endothelium-dependent relaxation to ACh, associated with increased vascular ROS production.²⁴ Conversely, the opposite effect was observed in female CETP

mice: decreased ROS and increased NO production, preserved vascular relaxation to ACh, and increased relaxation response to estrogen. These findings were associated with the activation of the ER α non-genomic pathway.²⁵ Here, we demonstrate that this sexual dimorphism mediated by CETP extends to the PVAT function. Since CETP-induced systemic phenotypes (CETP plasma activity and lipoprotein profile) are similar in both sexes, the sex-dependent CETP effects on the PVAT function are likely locally defined and independent of CETP plasma action, such as decreased HDL-C levels.

Male CETP mice exhibit a substantial loss of PVAT anticontractile effect. This effect was associated with local reduced NO levels and eNOS gene and protein expression, as well as oxidative stress. Conversely, female CETP mice did not display any impairment of the PVAT anticontractile function and showed increased NO and phospho-eNOS, and no changes in DHE fluorescence. It is possible that, in male CETP mice, eNOS uncoupling occurs, since the non-selective NOS inhibitor L-NAME abolished the elevation of DHE fluorescence in PVAT from male CETP mice. Uncoupled eNOS generates superoxide anion (O $_2^{\bullet-}$), which rapidly reacts with NO to form the hazardous peroxynitrite radical (ONOO $^-$).^{38,39} The functional significance of the adipocyte eNOS for vascular function was recently

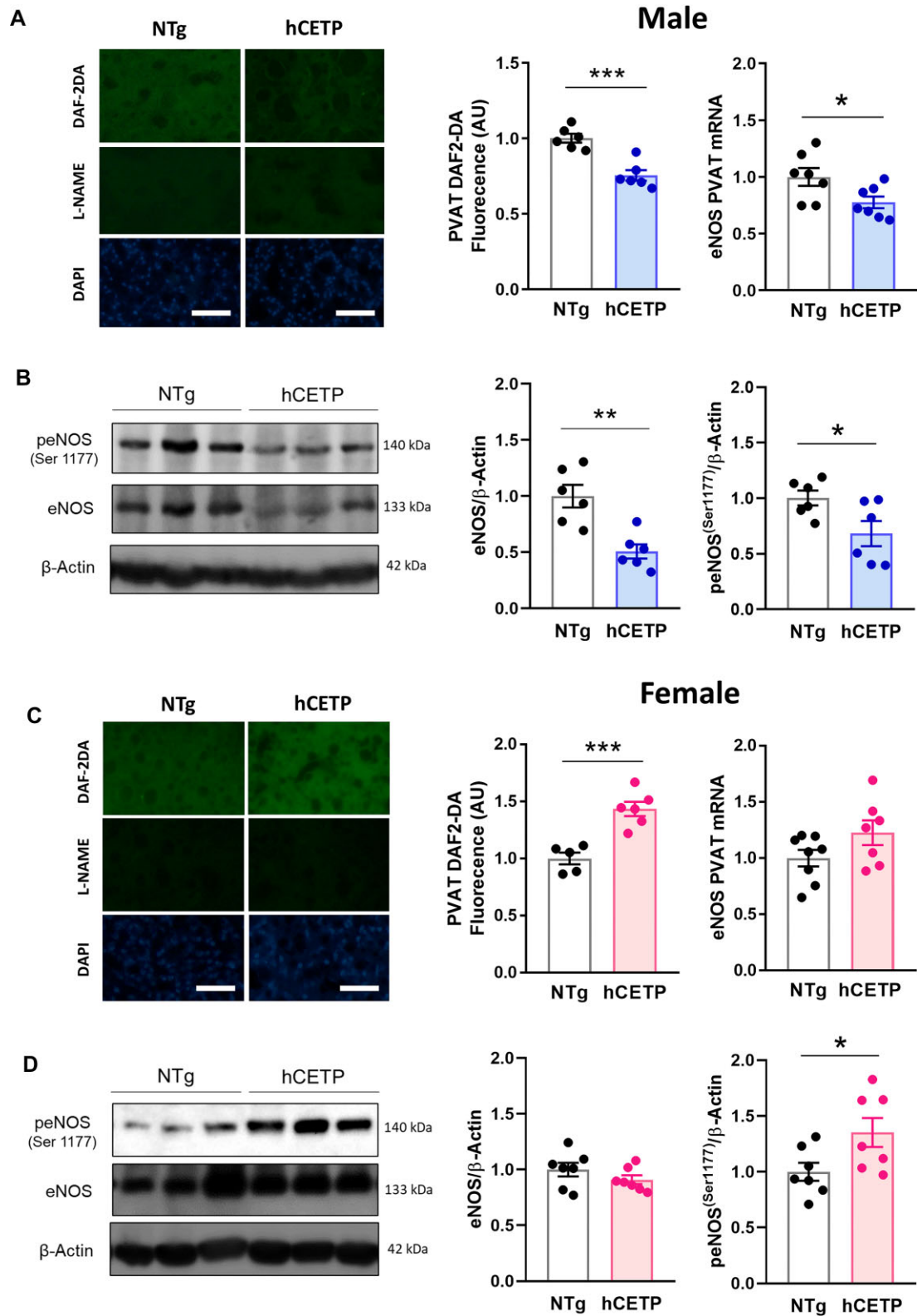


Figure 3. CETP expression modulates NO levels, eNOS expression, and phosphorylation in a sex-dependent way. NO production and eNOS mRNA expression in PVAT from male (A) to female (C) NTg and hCETP mice. Representative image and quantification of eNOS and phospho-eNOS protein expression in PVAT from male (B) to female (D) NTg and hCETP mice. Nuclei were stained with DAPI. Scale bar = 100 μ m. Gene expression data are corrected by Rplp0 internal control and protein expression by β -actin protein levels. Data are mean \pm SE, expressed relative to NTg controls (fold change). * $P \leq .05$, ** $P \leq .01$ and *** $P \leq .001$ by the Student's t test.

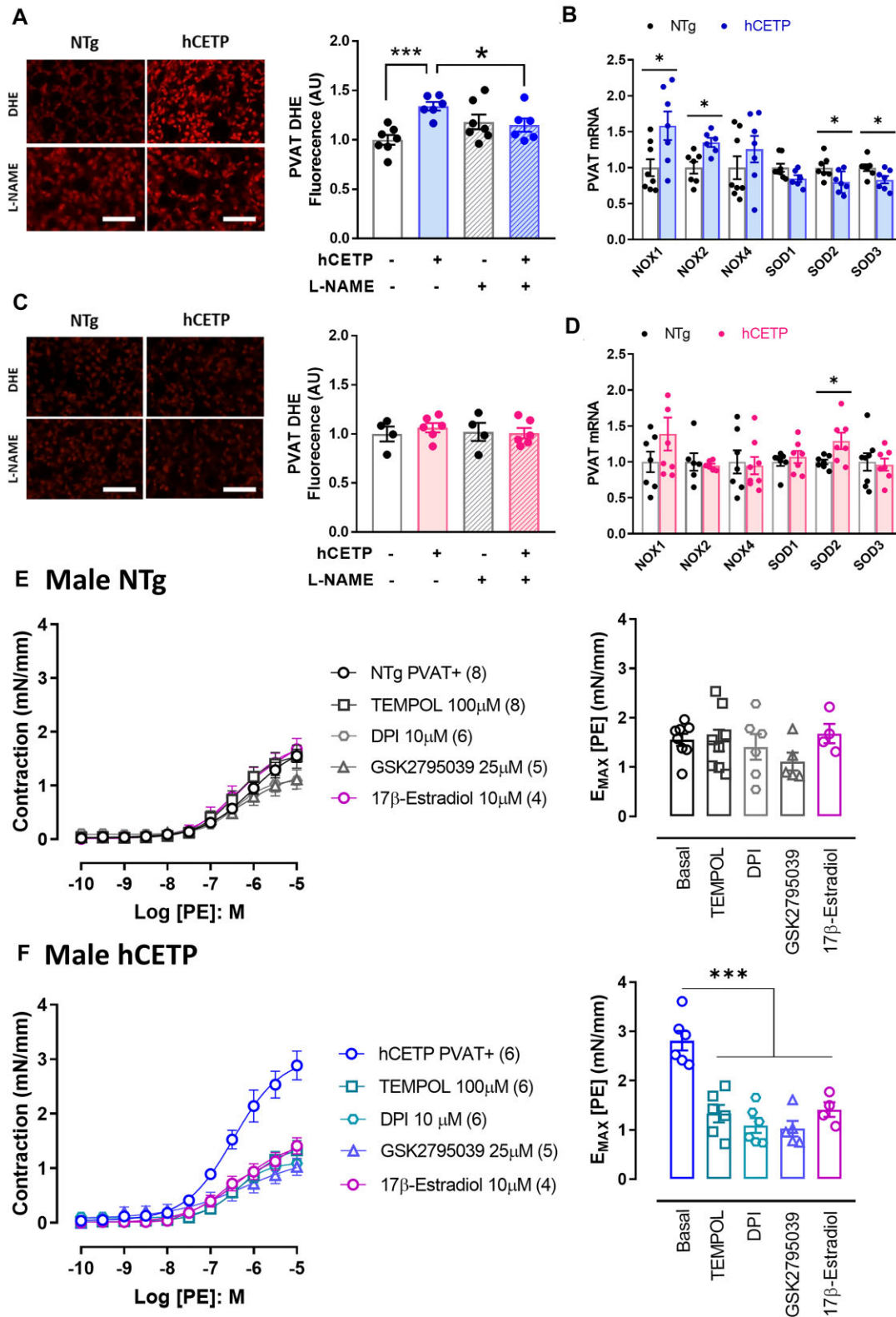


Figure 4. CETP expression induces oxidative stress in PVAT from males only, while NOX inhibition as well as SOD mimetic and 17 β -estradiol restore the PVAT anticontractile function in CETP male mice. DHE fluorescence was evaluated in PVAT with or without the NOS inhibitor (L-NAME) in male (A) and female (C) NTg and hCETP mice. mRNA expression of NADPH oxidase subunits NOX1, NOX2 (*Cybb*), and NOX4, as well as superoxide dismutase (SOD) 1, 2, and 3, were evaluated in PVAT from male (B) and female (D) NTg and hCETP mice. Concentration-response curves to phenylephrine (PE) in aortas with PVAT+, with or without NOX nonspecific inhibitor DPI, NOX2 specific inhibitor GSK2795039, SOD mimetic TEMPOL, and 17 β -Estradiol in male NTg (E) and male hCETP mice (F). Bar graphs represent maximum responses (E_{max}) to PE in NTg (E) and hCETP (F) males. Nuclei were stained with DAPI. Scale bar = 100 μ m. Gene expression data are corrected by the Rplp0 internal control. Data are mean \pm SE, expressed relative to NTg controls (fold change). A to D * P \leq .05 and *** P \leq .001 by Student's t-test. E and F *** P \leq .001 by one-way ANOVA.

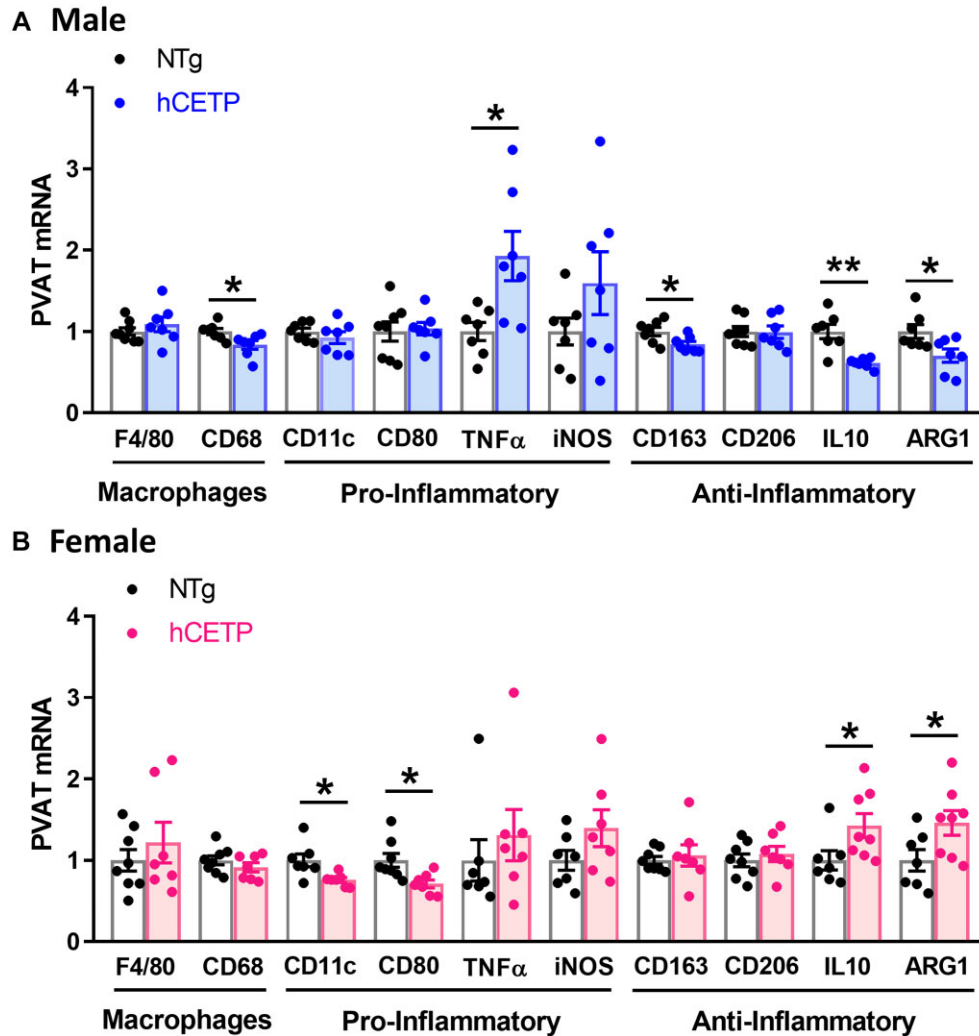


Figure 5. CETP expression induces sex-specific effects on the expression of pro- and anti-inflammatory markers in the PVAT of male and female mice. mRNA expression of markers of general macrophages (F4/80, CD68), pro-inflammatory markers (CD11c, CD80, TNF- α , and iNOS), and anti-inflammatory markers (CD163, CD206, IL-10, and ARG1) in male NTg and hCETP mice (A) and female NTg and hCETP mice (B). Gene expression was corrected by the Rplp0 internal control. Data are mean \pm SE, expressed relative to NTg (fold change). * $P \leq .05$ and ** $P \leq .01$ by the Student's *t*-test.

elucidated. Man and colleagues⁴⁰ generated adipocyte-specific eNOS knockout mice and observed exacerbated vascular dysfunction and remodeling, as well as increased expression of inflammation markers in the PVAT.

Uncoupling of NOS may be triggered by ROS, such as O₂⁻ from other sources, such as NOX2, and thus, a vicious cycle of ROS production takes place driving local disturbances.^{41,42} We have previously reported elevated NOX2 in the aortas of males²⁴ and decreased NOX2 in females²⁵ expressing CETP compared to their respective NTg controls. Here, we observed increased NOX-1 and 2 expression and decreased SOD 2 and 3 expression in the CETP male PVAT, but not in the CETP female PVAT, suggesting a participation of NOX in the oxidative stress detected in males. Functional *ex vivo* experiments showed that inhibition of ROS-generating enzymes, particularly NOX2 and scavenging ROS, restored PVAT anticontractile function in males. NOX2 activity was shown to mediate increases in ROS and TNF- α release and subsequent aortic dysfunction and stiffness in obese males.⁴³ Therefore, PVAT NOX2 may act as an important ROS source in PVAT-mediated vascular complications of CETP male mice. *Ex vivo* pretreatment with estrogen also restored

the PVAT anticontractile function in male CETP mice. The mechanisms are likely to involve antioxidant, anti-inflammatory, and NO production stimulation actions of estrogens.⁴⁴ These results suggest that CETP male PVAT may have diminished ER sensitivity compared to NTg males, since the estrogen receptors expression are not different in CETP and NTg males.

CETP expression has been shown to favor the M2 macrophage anti-inflammatory phenotype in peritoneal and bone marrow-derived macrophages.^{17,19} Considering that, we searched for indicators of inflammation in the PVAT of males and females expressing CETP. PVAT from male CETP mice showed reduced general markers of macrophages (CD68), but increased expression of pro-inflammatory factors (TNF α and iNOS) and reduced anti-inflammatory markers (CD63, IL-10, and Arg-1). In agreement, a previous study showed that activation of macrophages into the M1 pro-inflammatory state during inflammation was associated with the loss of the anticontractile effect of PVAT in small arteries of male mice.²⁷ In contrast, the PVAT of CETP female mice displayed decreased expression of pro-inflammatory markers (CD11c and CD80) and increased

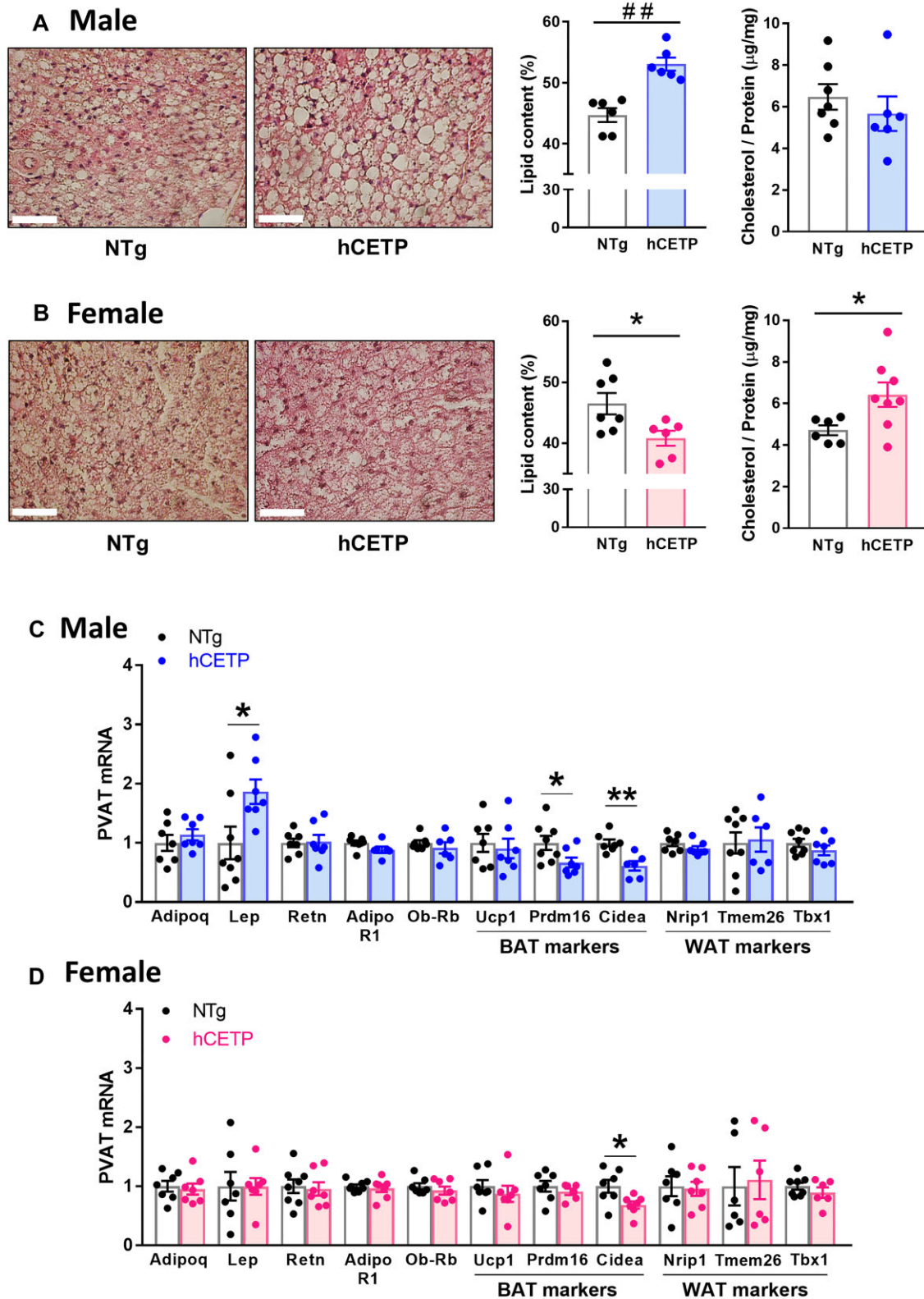


Figure 6. CETP expression induces sex-dependent alterations in PVAT morphology and adipose markers. PVAT adipocyte morphology by HE staining and quantification of fat area from male NTg to hCETP mice (A) and female NTg and hCETP mice (B). Gene expression of adipokines and its receptors and markers of brown (BAT) and white (WAT) adipocytes in PVAT from male NTg to hCETP mice (C) and female NTg to hCETP mice (D). Scale bar = 50 μ m. Typical images obtained with a 40 \times objective. Gene expression is relative to Rplp0 control. Data are mean \pm SE in % area or fold-change. * $P \leq .05$ and ** $P \leq .01$ by the Student's t-test. ## $P \leq .01$ by Mann-Whitney. Abbreviations: *Adipoq*: adiponectin, *Lep*: leptin, *Retn*: resistin, *AdipoR1*: adiponectin receptor 1, *Ob-rb* (*Lepr*): leptin receptor long form, *Ucp-1*: uncoupling Protein 1, *Prdm16*: PR/SET Domain 16, *Cidea*: cell death inducing DFFA like effector A, *Nrip1*: nuclear receptor interacting protein 1, *Tmem26*: transmembrane protein 26, *Tbx1*: tata-box transcription factor 1.

expression of anti-inflammatory effectors (Arg-1 and IL-10). This anti-inflammatory PVAT profile in females is possibly induced by estrogens. In aortas from atherosclerotic-prone *Apoe* knockout female mice, ovariectomy upregulates gene expression of F4/80 macrophage marker and proinflammatory markers NF- κ B, IL6R, VCAM1, and ICAM1.⁴⁵ In addition, aortic PVAT from female Sprague-Dawley rats expresses more M2-like macrophages than males in response to a high-fat diet.⁴⁶

By comparing morphology, lipid content, and key adipose tissue markers in the PVAT from male to female mice expressing CETP, we observed contrasting sex effects of CETP. PVAT from male CETP mice shows increased lipid droplet size and lipid content, while PVAT from female CETP mice presents reduced lipid and increased cholesterol contents. The female PVAT phenotype is in accordance with a previous report of diminished overall body adiposity due to increased lipolysis in white and brown (BAT) adipose tissue and increased cholesterol content of BAT of CETP female mice.¹⁵ Membrane cholesterol content is reduced in enlarged adipocytes, such as those from obese models, and increased in lean adipocytes.⁴⁷ Reduced membrane cholesterol was associated with large adipocyte dysfunction by modulating the expression of genes involved not only in cholesterol traffic, but also in genes involved in energy metabolism (fatty acid synthase, GLUT 4, and UCP3) and in adipocyte-derived secretion products (TNF α , angiotensinogen, and IL-6).⁴⁷

Increased lipid content observed in the PVAT from male CETP mice is confirmed by the marked elevation in the expression of the leptin gene. Chronically elevated leptin levels show several detrimental effects on the cardiovascular system. These include oxidative stress, susceptibility to thrombus formation, vascular inflammation, and atherosclerosis.⁴⁸⁻⁵⁰ Upregulation of leptin and pro-inflammatory genes have been found in the aortic PVAT of obese male mice, together with eNOS uncoupling, reduced NO levels, oxidative stress, and loss of the anticontractile action of PVAT,³³ similar to the results observed in male CETP mice in the present study. The increase in leptin expression was not found in PVAT from female CETP mice. As ovariectomy causes a significant increase in aortic PVAT leptin expression,⁴⁵ and CETP increases vascular effects of estrogen,²⁵ it is plausible to speculate that female hormones limit PVAT leptin expression.

Since CETP mediates sex-specific alterations in PVAT lipid content, we screened for the expression of key genes involved in lipid accumulation or depletion processes, such as adipogenesis and lipolysis. However, no sex-specific changes in the chosen genes were detected. Regarding gene markers of BAT, we observed a reduction of *Cidea* in the PVAT of both sexes expressing CETP, and a decrease in the *Prdm16* was observed in CETP males only. *Cidea* encodes a lipid droplet-associated protein and permits their enlargement. In cells that do not express this protein, various small lipid droplets are observed.⁵¹ This finding is, thus, associated with CETP expression and not with CETP sex-specific effects. This is also in agreement with the previous report on the attenuating effect of CETP on adiposity.¹⁵ In male CETP PVAT, the decrease of *Prdm16* may be responsible for the attenuation of the BAT-like phenotype of this tissue. The *Prdm16* gene serves as a transcriptional co-regulator crucial for the development of brown adipocytes⁵² and is considered a hallmark in beige adipose tissue.⁵²⁻⁵⁴ Silencing *Prdm16* induces “whitening” phenotype and exacerbates inflammation with macrophage activation in PVAT, impairing vascular remodeling following injury in male and ovariectomized female mice.⁵⁵ Consequently, the reduction of *Prdm16* expression in male CETP PVAT suggests that CETP induces “whitening” of this tissue in males.

Altogether, these data indicate that the effect of CETP on the PVAT phenotype and function is sex dependent. While CETP males exhibit impaired PVAT anti-contractile function, accompanied by oxidative stress, inflammation, and whitening, in females, CETP expression induced increased NO levels, anti-inflammatory phenotype, and preserved anti-contractile function. Thus, CETP imposes a sexual dimorphism on the PVAT regulation of vascular tonus, increasing CVD risk in males.

Acknowledgments

The representative histological images for this study were captured using the Upright Brightfield Microscope, available at the National Institute of Science and Technology on Photonics Applied to Cell Biology (INFABIC) and the Universidade Estadual de Campinas (UNICAMP). We thank the access to the equipment and assistance provided; INFABIC is co-funded by Fundação de Amparo à Pesquisa do Estado de São Paulo (FAPESP) (08/57906-3) and Conselho Nacional de Desenvolvimento Científico e Tecnológico (CNPq) (573913/2008-0). We are also grateful to Leandro Henrique de Paula Assis for technical assistance in qRT-PCR protocols.

Author Contributions

C.M.L.: investigation, methodology, visualization, formal analysis, writing—original draft; I.N.F., V.S.N., D.M.G.: investigation, formal analysis; J.A.V.: methodology, writing—review & editing; H.C.F.O., A.P.D.: conceptualization, methodology, resources, writing—review & editing, supervision, project administration, funding acquisition.

Supplementary Material

Supplementary material is available at the *APS Function* online.

Funding

This work was supported by grants from the Fundação de Amparo à Pesquisa do Estado de São Paulo (FAPESP) to H.C.F.O. (#2013/07607-8 and #2017/17728-8) and to A.P.D. (#2018/26080-4 and #2020/09799-5). Authors were supported by FAPESP fellowships 2019/13862-7 to C.M.L. and 2019/15164-5 to I.N.F.

Conflict of Interest

The authors declare that they have no competing interests.

Data Availability

The data that support the findings of this study are available from the corresponding author upon reasonable request.

References

- Hillock-Watling C, Gotlieb AI. The pathobiology of perivascular adipose tissue (PVAT), the fourth layer of the blood vessel wall. *Cardiovasc Pathol* 2022;**61**(Nov-Dec): 107459.
- Chang L, Garcia-Barrio MT, Chen YE. Perivascular adipose tissue regulates vascular function by targeting vascular smooth muscle cells. *ATVB* 2020;**40**(5):1094–1109.
- Li X, Ma Z, Zhu YZ. Regional heterogeneity of perivascular adipose tissue: morphology, origin, and secretome. *Front Pharmacol* 2021;**22**(12): 697720.

4. Soltis EE, Cassis LA. Influence of perivascular adipose tissue on rat aortic smooth muscle responsiveness. *Clin Exp Hypertens A* 1991;13(2):277–296.
5. Fésüs G, Dubrovska G, Gorzelniak K, et al. Adiponectin is a novel humoral vasodilator. *Cardiovasc Res* 2007;75(4):719–727.
6. Gao YJ, Zeng ZH, Teoh K, et al. Perivascular adipose tissue modulates vascular function in the human internal thoracic artery. *J Thorac Cardiovasc Surg* 2005;130(4):1130–1136.
7. Fitzgibbons TP, Kogan S, Aouadi M, et al. Similarity of mouse perivascular and brown adipose tissues and their resistance to diet-induced inflammation. *Am J Physiol Heart Circ Physiol* 2011;301(4):H1425–H1437.
8. Padilla J, Jenkins NT, Vieira-Potter VJ, et al. Divergent phenotype of rat thoracic and abdominal perivascular adipose tissues. *Am J Physiol-Regul, Integr Comp Physiol* 2013;304(7):R543–R552.
9. Drayna D, Jarnagin AS, McLean J, et al. Cloning and sequencing of human cholesteryl ester transfer protein cDNA. *Nature* 1987;327(6123):632–634.
10. Jiang XC, Moulin P, Quinet E, et al. Mammalian adipose tissue and muscle are major sources of lipid transfer protein mRNA. *J Biol Chem* 1991;266(7):4631–4639.
11. Tall A. Plasma lipid transfer proteins. *Annu Rev Biochem* 1995;64(1):235–257.
12. Kontush A. HDL-mediated mechanisms of protection in cardiovascular disease. *Cardiovasc Res* 2014;103(3):341–349.
13. Oliveira HCF, Raposo HF. Cholesteryl ester transfer protein and lipid metabolism and cardiovascular diseases. *Adv Exp Med Biol* 2020;1276:15–25.
14. Izem L, Greene DJ, Bialkowska K, et al. Overexpression of full-length cholesteryl ester transfer protein in SW872 cells reduces lipid accumulation. *J Lipid Res* 2015;56(3):515–525.
15. Raposo HF, Forsythe P, Chausse B, et al. Novel role of cholesteryl ester transfer protein (CETP): attenuation of adiposity by enhancing lipolysis and brown adipose tissue activity. *Metabolism* 2021;114(Jan): 154429.
16. Venancio TM, Machado RM, Castoldi A, et al. CETP lowers TLR4 expression which attenuates the inflammatory response induced by lps and polymicrobial sepsis. *Mediators Inflamm* 2016;2016:2016 1784014.
17. Santana KG, Righetti RF, Breda CNS, et al. Cholesterol-ester transfer protein alters M1 and M2 macrophage polarization and worsens experimental elastase-induced pulmonary emphysema. *Front Immunol* 2021;21(12): 684076.
18. Rentz T, Dorighello GG, Dos Santos RR, et al. CETP expression in bone-marrow-derived cells reduces the inflammatory features of atherosclerosis in hypercholesterolemic mice. *Biomolecules* 2023 Oct 22;13(10):1556.
19. Dorighello GG, Assis LHP, Rentz T, et al. Novel role of CETP in macrophages: reduction of mitochondrial oxidants production and modulation of cell immune-metabolic profile. *Antioxidants* 2022;11(9):1734.
20. Colhoun HM, Scheek LM, Rubens MB, et al. Lipid transfer protein activities in type 1 diabetic patients without renal failure and nondiabetic control subjects and their association with coronary artery calcification. *Diabetes* 2001;50(3):652–659.
21. Asztalos BF, Swarbrick MM, Schaefer EJ, et al. Effects of weight loss, induced by gastric bypass surgery, on HDL remodeling in obese women. *J Lipid Res* 2010;51(8):2405–2412.
22. Cappel DA, Palmisano BT, Emfinger CH, et al. Cholesteryl ester transfer protein protects against insulin resistance in obese female mice. *Mol Metab* 2013;2(4):457–467.
23. Zhu L, An J, Chinnarasu S, et al. Expressing the human cholesteryl ester transfer protein minigene improves diet-induced fatty liver and insulin resistance in female mice. *Front Physiol* 2021;12:799096.
24. Wanschel ACBA, Guizoni DM, Lorza-Gil E, et al. The presence of cholesteryl ester transfer protein (CETP) in endothelial cells generates vascular oxidative stress and endothelial dysfunction. *Biomolecules* 2021;11(1):69.
25. Lazaro CM, Victorio JA, Davel AP, et al. CETP expression ameliorates endothelial function in female mice through estrogen receptor- α and endothelial nitric oxide synthase pathway. *Am J Physiol Heart Circ Physiol* 2023;325(3):H592–H600.
26. Greenstein AS, Khavandi K, Withers SB, et al. Local inflammation and hypoxia abolish the protective anticontractile properties of perivascular fat in obese patients. *Circulation* 2009;119(12):1661–1670.
27. Withers SB, Agabiti-Rosei C, Livingstone DM, et al. Macrophage activation is responsible for loss of anticontractile function in inflamed perivascular fat. *ATVB* 2011;31(4):908–913.
28. Baltieri N, Guizoni DM, Victorio JA, et al. Protective role of perivascular adipose tissue in endothelial dysfunction and insulin-induced vasodilatation of hypercholesterolemic LDL receptor-deficient mice. *Front Physiol* 2018; 19(9): 229.
29. Parlee SD, Lentz SI, Mori H, MacDougald OA. Quantifying size and number of adipocytes in adipose tissue. *Methods Enzymol* 2014;2014(537):93–122.
30. Nunes VS, Leança CC, Panzoldo NB, et al. HDL-C concentration is related to markers of absorption and of cholesterol synthesis: study in subjects with low vs. high HDL-C. *Clin Chim Acta* 2011;412(1–2):176–180.
31. Marotti KR, Castle CK, Boyle TP, Lin AH, Murray RW, Melchior GW. Severe atherosclerosis in transgenic mice expressing simian cholesteryl ester transfer protein. *Nature* 1993;364(6432):73–75.
32. Saito T, Kurazumi H, Suzuki R, et al. Perivascular adipose tissue is a major source of nitric oxide in saphenous vein grafts harvested via the no-touch technique. *JAHA* 2022;11(3):e020637.
33. Xia N, Horke S, Habermeier A, et al. Uncoupling of endothelial nitric oxide synthase in perivascular adipose tissue of diet-induced obese mice. *ATVB* 2016;36(1):78–85.
34. Daiber A, Xia N, Steven S, et al. New therapeutic implications of endothelial nitric oxide synthase (enos) function/dysfunction in cardiovascular disease. *Int J Mol Sci* 2019;20(1):187.
35. Agabiti-Rosei C, Paini A, De Ciuceis C, et al. Modulation of vascular reactivity by perivascular adipose tissue (PVAT). *Curr Hypertens Rep* 2018;20(5):44.
36. Contreras GA, Thelen K, Ayala-Lopez N, et al. The distribution and adipogenic potential of perivascular adipose tissue adipocyte progenitors is dependent on sexual dimorphism and vessel location. *Physiol Rep* 2016;4(19):e12993.
37. Merone L, Tsey K, Russell D, et al. Sex inequalities in medical research: a systematic scoping review of the literature. *Women's Health Rep* 2022;3(1):49–59.
38. Piacenza L, Zeida A, Trujillo M, et al. The superoxide radical switch in the biology of nitric oxide and peroxynitrite. *Physiol Rev* 2022;102(4):1881–1906.
39. Kietadisorn R, Juni RP, Moens AL. Tackling endothelial dysfunction by modulating NOS uncoupling: new insights into its pathogenesis and therapeutic possibilities. *Am J Physiol Endocrinol Metab* 2012;302(5):E481–E495.
40. Man AWC, Zhou Y, Reifenberg G, et al. Deletion of adipocyte NOS3 potentiates high-fat diet-induced hyperten-

- sion and vascular remodeling via chemerin. *Cardiovasc Res* 2023;**119**(17):2755–2769.
41. Förstermann U, Münzel T. Endothelial nitric oxide synthase in vascular disease: from marvel to menace. *Circulation* 2006;**113**(13):1708–1714.
 42. Judkins CP, Diep H, Broughton BR, et al. Direct evidence of a role for Nox2 in superoxide production, reduced nitric oxide bioavailability, and early atherosclerotic plaque formation in ApoE^{-/-} mice. *Am J Physiol Heart Circ Physiol* 2010;**298**(1):H24–H32.
 43. DeVallance E, Branyan KW, Lemaster K, et al. Aortic dysfunction in metabolic syndrome mediated by perivascular adipose tissue TNF α - and NOX2-dependent pathway. *Exp Physiol* 2018;**103**(4):590–603.
 44. Nişã AR, Knock GA, Heads RJ. Signalling mechanisms in the cardiovascular protective effects of estrogen: with a focus on rapid/membrane signalling. *Curr Res Physiol* 2021; **28**(4): 103–118.
 45. Sun B, Yang D, Yin YZ, et al. Estrogenic and anti-inflammatory effects of pseudoprotodioscin in atherosclerosis-prone mice: insights into endothelial cells and perivascular adipose tissues. *Eur J Pharmacol* 2020;**15**(869): 172887.
 46. Kumar RK, Yang Y, Contreras AG, et al. Phenotypic changes in T cell and macrophage subtypes in perivascular adipose tissues precede high-fat diet-induced hypertension. *Front Physiol* 2021;**17**(12): 616055.
 47. Le Lay S, Krief S, Farnier C, et al. Cholesterol, a cell size-dependent signal that regulates glucose metabolism and gene expression in adipocytes. *J Biol Chem* 2001;**276**(20):16904–16910.
 48. Knudson JD, Dincer UD, Zhang C, et al. Leptin receptors are expressed in coronary arteries, and hyperleptinemia causes significant coronary endothelial dysfunction. *Am J Physiol Heart Circ Physiol* 2005;**289**(1):H48–H56.
 49. Sanches PL, de Mello MT, Elias N, et al. Hyperleptinemia: implications on the inflammatory state and vascular protection in obese adolescents submitted to an interdisciplinary therapy. *Inflammation* 2014;**37**(1):35–43.
 50. Raman P, Khanal S. Leptin in atherosclerosis: focus on macrophages, endothelial and smooth muscle cells. *Int J Mol Sci* 202;**22**(11):15446.
 51. Barneda D, Planas-Iglesias J, Gaspar ML, et al. The brown adipocyte protein CIDEA promotes lipid droplet fusion via a phosphatidic acid-binding amphipathic helix. *eLife* 2015;**26**(4): e07485.
 52. Seale P, Kajimura S, Yang W, et al. Transcriptional control of brown fat determination by PRDM16. *Cell Metab* 2007;**6**(1):38–54.
 53. Shapira SN, Seale P. Transcriptional control of brown and beige fat development and function. *Obesity* 2019;**27**(1):13–21.
 54. Wang Q, Li H, Tajima K, et al. Post-translational control of beige fat biogenesis by PRDM16 stabilization. *Nature* 2022;**609**(7925):151–158.
 55. Adachi Y, Ueda K, Nomura S, et al. Beiging of perivascular adipose tissue regulates its inflammation and vascular remodeling. *Nat Commun* 2022;**13**(1):5117.